

## ZnO Nanostructure Synthesized by Hydrothermal Method for Butane Gas Sensor

Abrar Ismardi <sup>a,\*</sup>, Vivia Puji Lestari <sup>a</sup>, Nor Hakim Abdullah <sup>b</sup>, Indra Wahyudin Fathona <sup>a</sup>,  
Theresia Deviyana Gunawan <sup>a</sup>

<sup>a</sup> Department of Engineering Physics, Telkom University, Jl. Telekomunikasi No.1 Terusan Buah Batu, Bandung, 40257, Indonesia

<sup>b</sup> Faculty of Bioengineering and Technology, Universiti Malaysia Kelantan Jeli Campus, 17600, Jeli, Kelantan, Malaysia

Corresponding author: \*[abrarselah@telkomuniversity.ac.id](mailto:abrarselah@telkomuniversity.ac.id)

**Abstract**— Zinc oxide (ZnO) nanostructure was successfully synthesized on an alumina substrate by the hydrothermal method. The hydrothermal method consists of two stages: the preparation of seeding layers and the growth of ZnO nanostructures. 0.4 M Zinc Acetate Dihydrate ( $\text{Zn}(\text{CH}_3\text{COO})_2 \cdot 2\text{H}_2\text{O}$ ) and 3 M Sodium Hydroxide (NaOH) were used as precursors. The hydrothermal process was carried out at 90 °C for 4 hours. Morphological characterization of ZnO nanostructures was conducted by using Scanning Electron Microscope (SEM). The result produces a diameter of 60-80 nm and a length of 600-800 nm in the form of nanoflowers. The crystal and crystalline structure were studied with XRD, and it was shown that the ZnO nanostructure is a wurtzite structure in the form of a hexagonal shape and has a crystallite size of 59 nm. After conducting electrical characterization, it was shown that the current is directly proportional to the voltage, forming an ohmic contact curve. ZnO nanostructures have the potential to be applied as a gas sensor since the good response indicated the presence of butane gas. It is clarified that the nanostructure with a flow rate of 200 mL/min has a change in resistance of 0.17 M $\Omega$ /s with a recovery time of 30 seconds when it is exposed to butane gas for one minute. ZnO nanostructures also have a sensitivity change of 0.000495 M $\Omega$ /mL in the gas flow rate range of 50-250 mL/min.

**Keywords**— ZnO; hydrothermal; nanostructure; nanoflowers; gas sensor; butane classification numbers: 6.08.

Manuscript received 19 Nov. 2022; revised 16 Mar. 2023; accepted 20 Apr. 2023. Date of publication 30 Jun. 2023.  
IJASEIT is licensed under a Creative Commons Attribution-Share Alike 4.0 International License.



### I. INTRODUCTION

Zinc oxide (ZnO) is one of the most popular metal oxide semiconductors that has a wide band gap (3.37 eV) and large exciton binding energy (60 meV) [1]. ZnO in nanostructures has become very interesting to researchers compared to its bulk condition to its high surface and volume ratio [2]. The peculiar properties of ZnO nanostructures have been applied to some applications, especially gas sensors [3]. ZnO has been widely used as a gas sensor due to its high selectivity and sensitivity when exposed to the gas, even at very small concentrations. [4]. Many gases have been tried to be sensed by ZnO nanostructure. Different nanostructures have been synthesized for detecting some gases, i.e., acetone [5], ethanol [6], NH<sub>3</sub> [7], LPG [8], and methanol [9]. All of the ZnO nanostructures were synthesized by thermal oxidation [10], thermal decomposition [11], co-precipitation method [12], liquid phase reaction [13], a self-template method [14], a solvothermal method [15], electrodeposition method [16], a microwave-assisted method [17] and many other methods.

Among them, there was no report about using the hydrothermal method for the synthesis of ZnO nanostructure. Comparing to the method describe before, the hydrothermal method is one of the simple and cheapest way to synthesis ZnO nanostructure [18], there were no need advance instrument, and the result can be controlled easily. Besides that, there were not many reports regarding the usage of ZnO nanostructures to be applied for the detection of butane gas. One of them reported the usage of a thin film of ZnO for butane gas sensing [19].

Air pollution has become one of the main problems in the world, especially in developing countries. There are many sources of air pollution, i.e., vehicle gas emissions, factories, and other sources, especially in a big city. One of flammable gas can be found around home is butane that is usually used for cooking [20]. Leakage detection of butane should be possible using a very sensitive gas sensor, even at very low gas concentrations. A good air quality management system is a must to be used, since good air quality is a must, there are many sensors to be developed, especially butane gas sensors.

Many gas sensor systems have been developed worldwide; the current need in gas sensors is a sensor with high selectivity, high sensitivity, and fast response and recovery times. The gas sensor based on nanostructure material will be the most promising application [21]. Metal oxide semiconductors are used to fabricate nanosensor gases because they have high sensitivity and can be facilitated with good, easily fabricated, and inexpensive gases [22]. The metal oxide semiconductor materials used as gas sensors are ZnO [23], SnO<sub>2</sub> [24], WO<sub>3</sub> [25], Ga<sub>2</sub>O<sub>3</sub> [26], TiO<sub>2</sub> [27] and Fe<sub>2</sub>O<sub>3</sub> [28]. Among these materials, ZnO is the material most widely developed by researchers. The advantages of ZnO are high electron mobility, large band gap energy, high extension energy, transparency to visible light, antibacterial, non-contradictory, and good thermal properties. [29].

This paper presents the synthesis of ZnO nanostructures using the hydrothermal method. The hydrothermal method is chosen since it is the simplest and cheapest way to synthesize nanostructured ZnO. Their morphology and crystallinity then characterized the nanostructure synthesized. Finally, it can be applied as a gas sensor for detecting butane gas.

## II. MATERIALS AND METHOD

The synthesis process begins with the stage of deposition of the seeding layer. The experiment begins with dissolving 1.976 grams of 0.3 M Zinc Acetate Dihydrate (Zn(O<sub>2</sub>CCH<sub>3</sub>)<sub>2</sub>(H<sub>2</sub>O)<sub>2</sub>) 99.99% from Merck (without further purification) into 20 mL of deionized water. The solution is stirred using a magnetic stirrer in a heated state until the temperature reaches 60 °C. The temperature was then maintained at 60 °C so the ZnAc solution became homogeneous. The seeding layer was then deposited by dipping the alumina substrate into the seeding solution for 5 minutes. After the dipping, the substrate was placed at the top of the aluminum foil container for baking at 110° C temperature for 15 minutes. This process aims to eliminate the ethanol content in the substrate.

In the next process, the hydrothermal solution was then prepared. 0.4 M, 99.99% Zinc Acetate Dihydrate (Zn(O<sub>2</sub>CCH<sub>3</sub>)<sub>2</sub>(H<sub>2</sub>O)<sub>2</sub>) powder from Merck, and 3M sodium Hydroxide (NaOH) pellets from Merck, 99.99% as precursors, were used without further purification. Each chemical was mixed with deionized water and stirred using a magnetic stirrer for 30 minutes. After being completely mixed, the two solutions were mixed into a 50 mL beaker to be stirred again using a magnetic stirrer for another 30 minutes. After the solution is complete, the solution is poured into a growth bottle. The selected growth bottles are Schott Duran bottles of 50 mL. A tin coil is attached to the bottle cap using duct tape foam and thermal tape as the media to put the substrate. The substrate that had been dipped with the seeding layer was then placed in a bottle cap with a hanging state. The position of the hanging substrate is expected to facilitate the hydrothermal process through the natural convection process by heat and gravity. Particles in the solution will easily rise to the top due to the addition of heat and pressure from the outside. The nanostructure crystallization process can occur on a hanging substrate. The synthesis process is continued by inserting the bottle into the oven with a heating temperature of 90 ° C for about 4 hours. After heating, the white layer on the substrate's surface was expected to be ZnO nanostructure. The substrate

was then washed using ethanol to remove the remaining zinc acetate attached to the substrate. The washing process was then followed by deionized water, as shown in the flowchart Fig. 1 below.

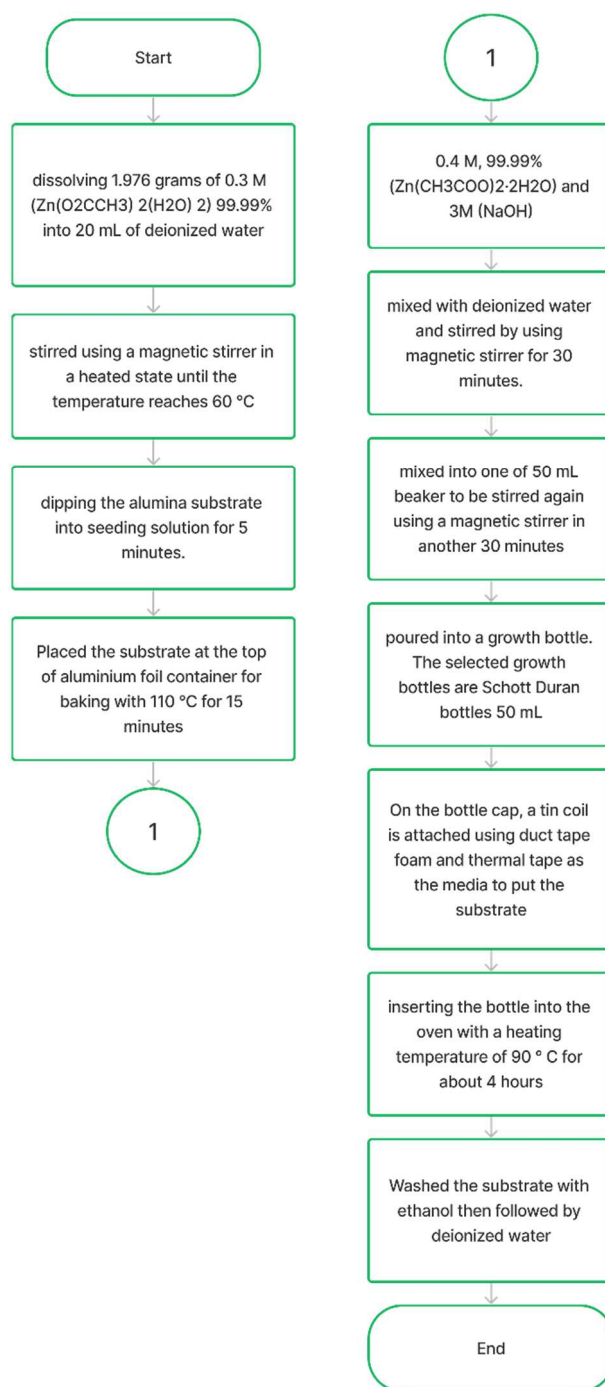


Fig. 1 The Synthesis Process of ZnO Nanostructure

## III. RESULTS AND DISCUSSION

Morphological characterization with Scanning Electron Microscopy (SEM) showed that the ZnO nanoflowers were grown in this process. Nanoflowers are another designation for nanostructures in the form of rods that resemble flowers. The results of this study are consistent with previous studies, which state that the synthesis of ZnO nanostructures using high pH or alkaline precursors such as NaOH or KOH will

produce nanostructures that resemble flowers[30]. Each ZnO nanorod is known to have diameters of 60-80 nm with lengths of 600-800 nm. The elemental confirmation inside the nanostructures was then tested with EDS. The results show that ZnO nanostructures only have material compositions from ZnO nanostructured samples consisting of Zn, O, C, and Na elements. There was no impurity found in this grown result. The dominant Zn content is 59.12%, and O of 13.96 indicates the sample is proven ZnO. The elements C and Na indicate that some elements in the precursor content are found during the synthesis process. SEM images and EDS results are shown in Fig. 2 below.

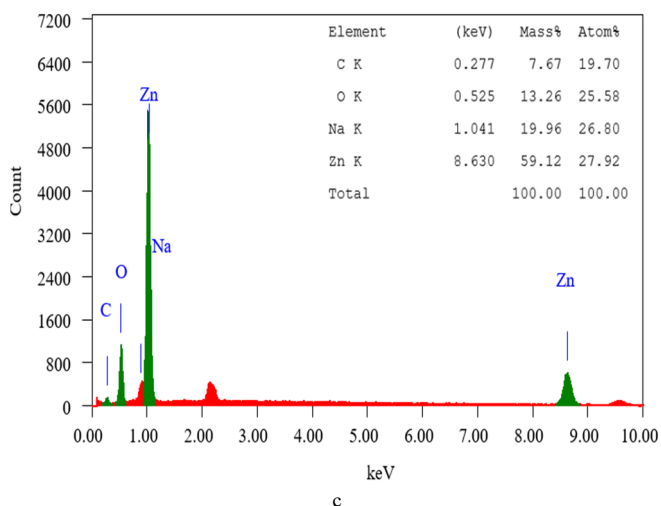
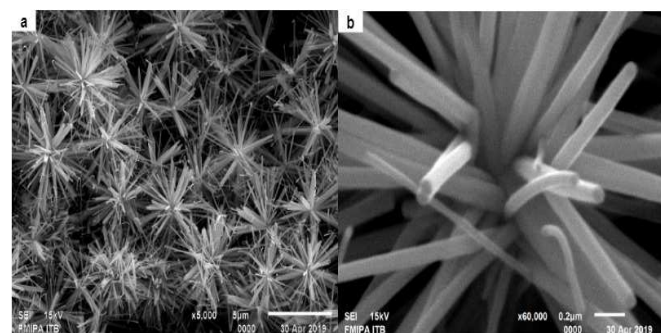


Fig. 2 (a) ZnO nanoflowers grown during the synthesis process, (b) the nanoflowers contains of single ZnO nanorod and formed nanoflowers and (c) the EDS result shows the elemental composition of the ZnO nanoflowers.

The crystallinity study of the grown ZnO nanoflowers was then conducted using X-Ray Diffraction (XRD). The peaks observed were sharp and narrow in shape, indicating that the sample formed a crystal structure. The results of the peaks correspond to the ZnO COD reference database [96-900-8877] (shown in the figure as a red line below the graph) in a 31.6° position with an orientation of (100), 35° at (002), 37.65° at (101) and 43.19° at (012) indicate the wurtzite crystalline ZnO structure in a hexagonal shape. The other peak corresponds to the Al<sub>2</sub>O<sub>3</sub> COD database [96-101-0915] (pictured here as a green line below the graph). These other peaks arise because the ZnO nanostructure is grown on an alumina substrate, so during XRD testing, the alumina substrate part is also diffracted by X-rays: 5,1232 Å. The diffraction pattern of ZnO nanostructures can be observed in Fig. 3.

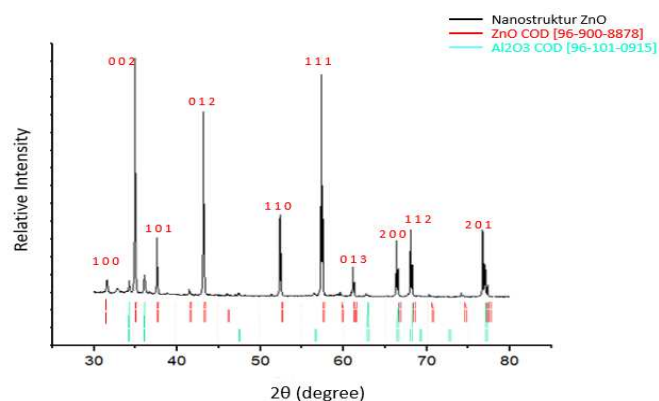


Fig. 3 XRD diffraction peak of as synthesized ZnO nanostructure.

A response test was carried out in the presence of butane gas to determine the potential of ZnO nanostructures as a gas sensor. Three of the best samples were selected based on the results of the electrical conductivity test with the best linearity. The three best samples are ZnO nanostructures with 0.05 M 2 and 4 hours ZnO, respectively, continuing with a sample of 0.15 M 4 hours dipping in the seeding layer. All of the samples were deposited on the alumina substrate. Gas sensor testing was carried out by flowing butane gas at a 200 mL/minute flow rate. The changes in resistance indicate the sample's response to the presence of butane gas. The result is shown in Fig. 4 below. The response curve in Fig. 4 shows that the sample with a 0.05 M 4-hour dipping in the seeding layer shows the fastest change in resistance of 0.170 MΩ/s. The result follows the sample of 0.05 M 2 hours dipping in a seeding layer. It was 0.053 MΩ/s and the sample of 0.15 M dipping in seeding solution for 4 hours of 0.052 MΩ/s. All the samples were then exposed to butane gas for about 1 minute, and they had a relatively similar recovery time of about 30 seconds.

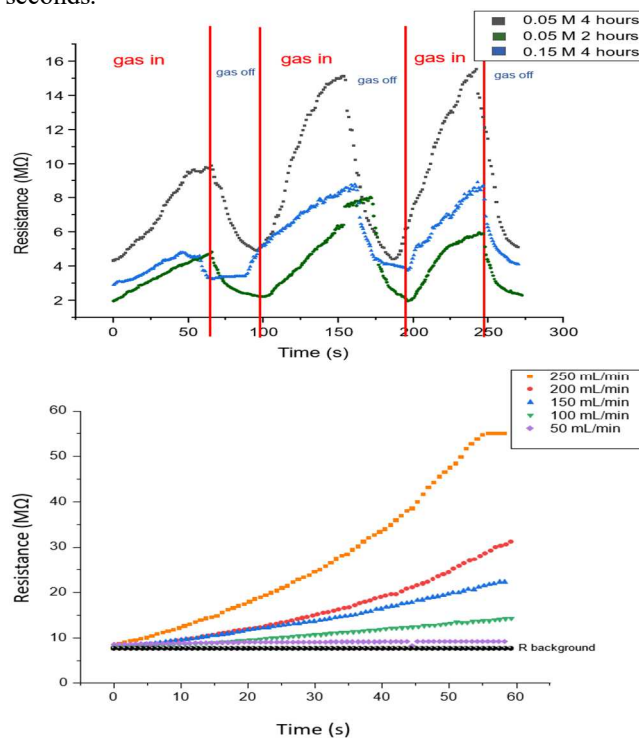


Fig. 4 (a) Response of ZnO nanostructure to the presence of butane gas for different dipping times to seeding solution, (b) the change of resistance with the relation of exposure time to butane gas.

Based on the graph in Fig. 4, it is concluded that the sensitivity value depends on the butane gas flow rate. The greater the flow rate of butane gas exposed to the sample, the higher the sensitivity value. The sample has a sensitivity change of 0,000495 MΩ/mL in the gas flow rate range of 50-250 mL/min. This shows that although the sample has a sensitivity change, the change in sensitivity is relatively not large even though the sample is exposed to various butane gas flow rates. The ZnO nanostructure sample has the opportunity to become a butane gas sensor. The graph of the change in sensitivity of the ZnO nanostructure to the butane gas flow rate is shown in Fig. 5.

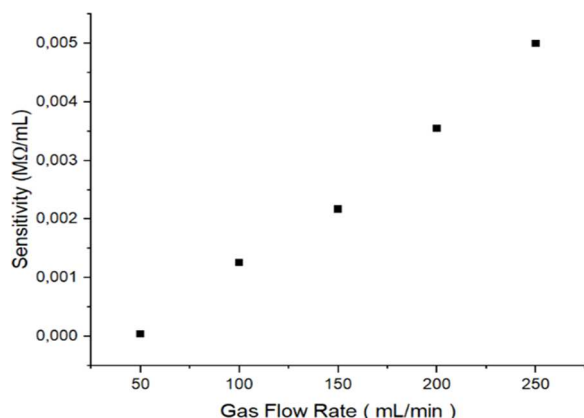


Fig. 5 Changes in the Sensitivity of ZnO Nanostructures to Butane Gas Flow Rates.

In general, the interaction of the sensing layer with the target gas to be detected can result in electrical resistance modulation, which can lead to gas detection based on semiconducting metal oxide (SMO). When SMO is exposed to air, oxygen molecules will adsorb on the sensor's surface due to the ionization of those molecules. The layer that results from the adsorption of oxygen molecules is known as the electron depletion layer, and it is characterized by a low electron concentration on the n-type SMO's surface and a high resistance to the metal oxide's core as shown in Fig. 6. The electron depletion layer and hole accumulation layer of the n-type SMO increase when an oxidizing gas is applied as the target gas in the sensing operation, raising resistance. The adsorption of target gas molecules in SMO also depends on the surface area, with variations in morphology leading to variable adsorption capacities. As a result, a gas sensor with a larger surface area will have more adsorption and a higher response [31].

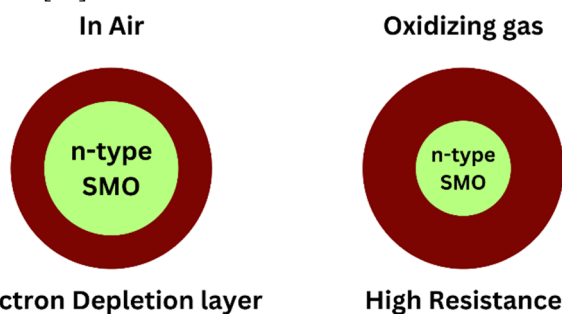


Fig. 6 Gas Sensing Mechanism in n-type SMO When Exposed to Oxidizing Gas

The gas detection process in this work is related to the principle of the SMO conductometric sensor, which involves adsorption and chemical reactions that occur between the gas target and the active surface, causing a change in resistance. SMO is employed in the form of ZnO, which is an n-type metal oxide. When ZnO surface layer interacts with air, oxygen molecules, which can be  $O^-$ ,  $O^{2-}$ , or  $O_2^-$  containing, adsorb the surface area of ZnO by attaching electrons in the ZnO conduction band. The molecule that leads to a depletion area on the surface of ZnO as shown in Fig. 7 and the reaction below, occurs in the presence of ZnO in ambient air [32, 33].

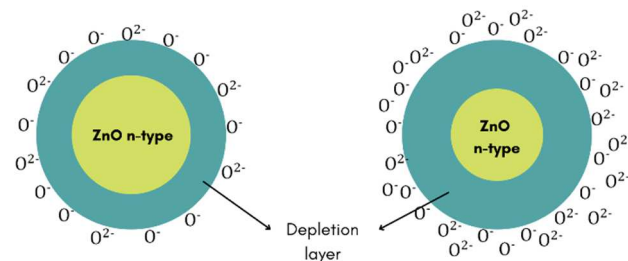
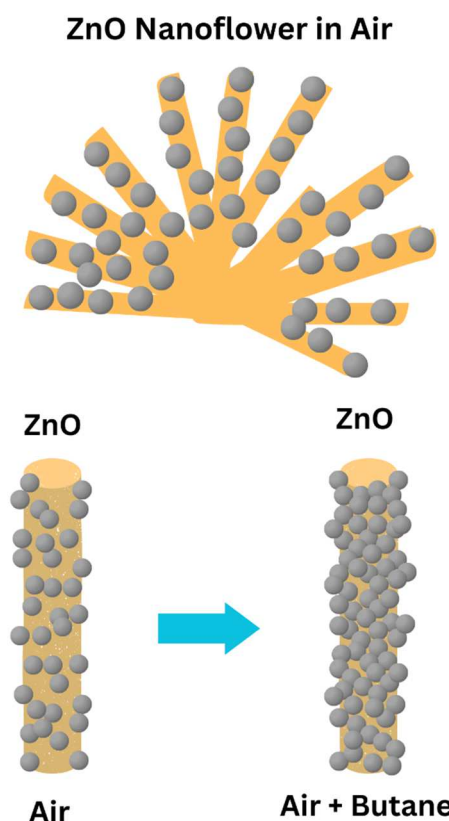
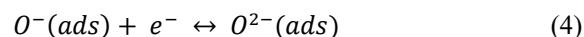
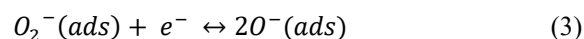
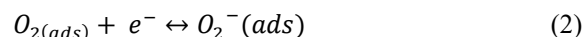


Fig. 7 ZnO Nanoflowers Gas Sensing Mechanism When Exposed Butane Gas Causes Change in Depletion Layer (a) ZnO Nanoflowers in air (b) ZnO with Oxygen Interact with Butane Gas (c) Depletion layer Change Caused by Butane gas

The absorbed oxygen molecules in ZnO will then react with butane gas ( $C_4H_{10}$ ) as shown in Fig. 7(b). The oxygen adsorption process reduces the conductive surface of ZnO. Butane's oxidation processes include dehydrogenization, isomerase, partial oxidation by breaking carbon bonds, and thorough oxidation and the sensing mechanism is explained by the reaction shown below and Fig. 8 [34].

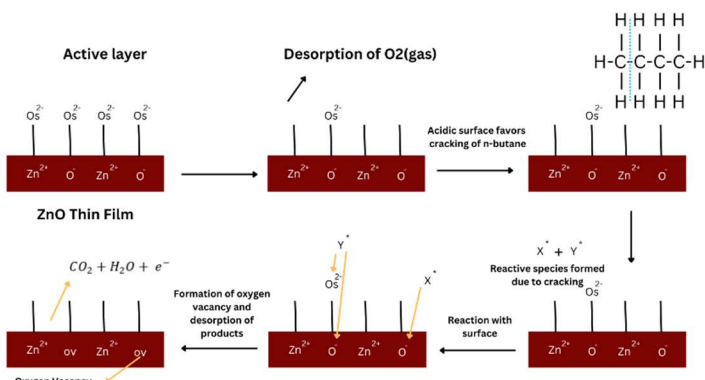
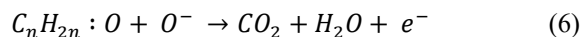
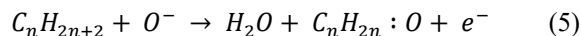


Fig. 8 Reaction Scheme of Butane Gas With Oxygen Surface

#### IV. CONCLUSION

The ZnO nanostructure was successfully synthesized by the hydrothermal method. The hydrothermal method is carried out in pre-treatment and hydrothermal stages. Pre-treatment is done by giving a 0.05 M seeding layer by the dip coating method. Hydrothermal synthesis was carried out using 0.4 M Zinc Acetate Dihydrate and 3 M NaOH in distilled water with a hydrothermal time of 4 hours, resulting in a small ZnO nanostructure with a uniform growth distribution. The results of morphological characterization using SEM produce ZnO nanostructures in the form of nanoflowers with diameters of 60-80 nm and lengths of 600-800 nm. The XRD result showed that the ZnO nanostructure has a hexagonal wurtzite crystal structure with a crystallite size of 59 nm and a lattice size of  $a$ : 3.26664 Å and  $c$ : 5.1232 Å. Electrical conductivity was then tested to study the effect of morphology on conductivity. The smaller the size and uniformly distributed growth of nanostructures, the higher the value of electrical conductivity. It is indicated by the decrease in the value of resistance and the form of an ohmic curve. The ZnO nanostructure has the potential to be applied as a gas sensor because it is responsive to the presence of butane gas. The gas sensor characteristic was characterized by a change in resistance of 0.17 MΩ / s at a gas flow rate of 200 mL/min with a recovery time of 30 seconds when exposed to butane gas for one minute. The ZnO nanostructure also has a sensitivity change of 0.000495 MΩ / mL in the gas flow rate range of 50-250 mL / min.

#### ACKNOWLEDGMENT

We thank Telkom University for the fully funded research under the international matching grant of 016/PNLT3/PPM/2020.

#### REFERENCES

- [1] S. Oh, T. H. Lee, M. S. Chae, J. H. Park, and T. G. Kim, "Performance improvements of ZnO thin film transistors with reduced graphene oxide-embedded channel layers," *J Alloys Compd*, vol. 777, pp. 1367–1374, Mar. 2019, doi: 10.1016/j.jallcom.2018.11.004.
- [2] S. Raha and M. Ahmaruzzaman, "ZnO nanostructured materials and their potential applications: progress, challenges and perspectives," *Nanoscale Advances*, vol. 4, no. 8. Royal Society of Chemistry, pp. 1868–1925, Mar. 09, 2022. doi: 10.1039/d1na00880c.
- [3] V. S. Bhati, M. Hojamberdiev, and M. Kumar, "Enhanced sensing performance of ZnO nanostructures-based gas sensors: A review," *Energy Reports*, vol. 6. Elsevier Ltd, pp. 46–62, Feb. 01, 2020. doi: 10.1016/j.egy.2019.08.070.
- [4] M. Aleksanyan, A. Sayunts, V. Aroutiounian, G. Shahkhatuni, Z. Simonyan, and G. Shahnazaryan, "Gas Sensor Based on ZnO Nanostructured Film for the Detection of Ethanol Vapor," *Chemosensors*, vol. 10, no. 7, Jul. 2022, doi: 10.3390/chemosensors10070245.
- [5] P. Wang, T. Dong, C. Jia, and P. Yang, "Ultrasensitive acetone-gas sensor based ZnO flowers functionalized by Au nanoparticle loading on certain facet," *Sens Actuators B Chem*, vol. 288, pp. 1–11, Jun. 2019, doi: 10.1016/j.snb.2019.02.095.
- [6] G. Ren *et al.*, "ZnO@ZIF-8 core-shell microspheres for improved ethanol gas sensing," *Sens Actuators B Chem*, vol. 284, pp. 421–427, Apr. 2019, doi: 10.1016/j.snb.2018.12.145.
- [7] G. H. Mhlongo, D. E. Motaung, F. R. Cummings, H. C. Swart, and S. S. Ray, "A highly responsive NH3 sensor based on Pd-loaded ZnO nanoparticles prepared via a chemical precipitation approach," *Sci Rep*, vol. 9, no. 1, Dec. 2019, doi: 10.1038/s41598-019-46247-z.
- [8] S. S. Nkosi *et al.*, "The effect of stabilized ZnO nanostructures green luminescence towards LPG sensing capabilities," *Mater Chem Phys*, vol. 242, Feb. 2020, doi: 10.1016/j.matchemphys.2019.122452.
- [9] A. Saaedi, P. Shabani, and R. Yousefi, "High performance of methanol gas sensing of ZnO/PANI nanocomposites synthesized under different magnetic field," *J Alloys Compd*, vol. 802, pp. 335–344, Sep. 2019, doi: 10.1016/j.jallcom.2019.06.088.
- [10] A. Rinaldi *et al.*, "A simple ball milling and thermal oxidation method for synthesis of ZnO nanowires decorated with cubic ZnO nanoparticles," *Nanomaterials*, vol. 11, no. 2, pp. 1–15, Feb. 2021, doi: 10.3390/nano11020475.
- [11] H. S. M. Abd-Rabboh, M. Eissa, S. K. Mohamed, and M. S. Hamdy, "Synthesis of ZnO by thermal decomposition of different precursors: Photocatalytic performance under UV and visible light illumination," *Mater Res Express*, vol. 6, no. 5, 2019, doi: 10.1088/2053-1591/ab04ff.
- [12] N. B. Mahmood, F. R. Saeed, K. R. Gbashi, and U. S. Mahmood, "Synthesis and characterization of zinc oxide nanoparticles via oxalate co-precipitation method," *Materials Letters: X*, vol. 13, Mar. 2022, doi: 10.1016/j.mlmlx.2022.100126.
- [13] R. Wang, "Liquid-Phase Synthesis of Nano-Zinc Oxide and Its Photocatalytic Property," *Int J Anal Chem*, vol. 2022, pp. 1–9, Jun. 2022, doi: 10.1155/2022/6977424.
- [14] G. Ren *et al.*, "ZnO@ZIF-8 core-shell microspheres for improved ethanol gas sensing," *Sens Actuators B Chem*, vol. 284, pp. 421–427, Apr. 2019, doi: 10.1016/j.snb.2018.12.145.
- [15] A. A. Ruba, L. M. Johny, N. S. Nirmala Jothi, and P. Sagayaraj, "ScienceDirect Solvothermal Synthesis, Characterization and Photocatalytic activity of ZnO Nanoparticle," 2019. [Online]. Available: www.sciencedirect.com
- [16] C. Wang *et al.*, "In situ synthesis of flower-like ZnO on GaN using electrodeposition and its application as ethanol gas sensor at room temperature," *Sens Actuators B Chem*, vol. 292, pp. 270–276, Aug. 2019, doi: 10.1016/j.snb.2019.04.140.
- [17] K. R. Ahammed *et al.*, "Microwave assisted synthesis of zinc oxide (ZnO) nanoparticles in a noble approach: utilization for antibacterial and photocatalytic activity," *SN Appl Sci*, vol. 2, no. 5, May 2020, doi: 10.1007/s42452-020-2762-8.
- [18] S. Mohan, M. Vellakkat, A. Aravind, and U. Reka, "Hydrothermal synthesis and characterization of Zinc Oxide nanoparticles of various shapes under different reaction conditions," *Nano Express*, vol. 1, no. 3, Dec. 2020, doi: 10.1088/2632-959X/abc813.
- [19] M. Aleksanyan, A. Sayunts, V. Aroutiounian, G. Shahkhatuni, Z. Simonyan, and G. Shahnazaryan, "Gas Sensor Based on ZnO Nanostructured Film for the Detection of Ethanol Vapor," *Chemosensors*, vol. 10, no. 7, Jul. 2022, doi: 10.3390/chemosensors10070245.

- [20] M. H. Asadiyan, S. Parhoodeh, and S. Nazem, "Simulation and fabrication of butane gas sensor based on surface plasmon resonance phenomenon," *Optik (Stuttg)*, vol. 256, Apr. 2022, doi: 10.1016/j.ijleo.2022.168738.
- [21] L. Ge, X. Mu, G. Tian, Q. Huang, J. Ahmed, and Z. Hu, "Current Applications of Gas Sensor Based on 2-D Nanomaterial: A Mini Review," *Frontiers in Chemistry*, vol. 7, Frontiers Media S.A., Dec. 10, 2019, doi: 10.3389/fchem.2019.00839.
- [22] A. Mirzaei, H. R. Ansari, M. Shahbaz, J. Y. Kim, H. W. Kim, and S. S. Kim, "Metal Oxide Semiconductor Nanostructure Gas Sensors with Different Morphologies," *Chemosensors*, vol. 10, no. 7, MDPI, Jul. 01, 2022, doi: 10.3390/chemosensors10070289.
- [23] M. A. Franco, P. P. Conti, R. S. Andre, and D. S. Correa, "A review on chemiresistive ZnO gas sensors," *Sensors and Actuators Reports*, vol. 4, Nov. 2022, doi: 10.1016/j.snr.2022.100100.
- [24] Y. Kong *et al.*, "SnO<sub>2</sub> nanostructured materials used as gas sensors for the detection of hazardous and flammable gases: A review," *Nano Materials Science*, 2021, doi: 10.1016/j.nanoms.2021.05.006.
- [25] J. Xiao *et al.*, "Synthesis of WO<sub>3</sub> nanorods and their excellent ethanol gas-sensing performance," *Materials Research*, vol. 24, no. 3, Mar. 2021, doi: 10.1590/1980-5373-MR-2020-0434.
- [26] A. Afzal, "β-Ga<sub>2</sub>O<sub>3</sub> nanowires and thin films for metal oxide semiconductor gas sensors: Sensing mechanisms and performance enhancement strategies," *Journal of Materiomics*, vol. 5, no. 4, Chinese Ceramic Society, pp. 542–557, Dec. 01, 2019, doi: 10.1016/j.jmat.2019.08.003.
- [27] J. Malallah Rzajj and A. Mohsen Abass, "Review on: TiO<sub>2</sub> Thin Film as a Metal Oxide Gas Sensor," *Journal of Chemical Reviews*, vol. 2, no. 2, pp. 114–121, Mar. 2020, doi: 10.33945/SAMI/JCR.2020.2.4.
- [28] P. Karnati1, A. Akbar1, and P. A. Morris1, "Conduction Mechanisms in One Dimensional Core-Shell Nanostructures for Gas Sensing: A Review," 2019.
- [29] D. K. Sharma, S. Shukla, K. K. Sharma, and V. Kumar, "A review on ZnO: Fundamental properties and applications," in *Materials Today: Proceedings*, Elsevier Ltd, 2020, pp. 3028–3035, doi: 10.1016/j.matpr.2020.10.238.
- [30] A. Klinbumrung, R. Panya, A. Pung-Ngama, P. Nasomjai, J. Saowalakmekka, and R. Sirirak, "Green synthesis of ZnO nanoparticles by pineapple peel extract from various alkali sources," *Journal of Asian Ceramic Societies*, vol. 10, no. 4, pp. 755–765, 2022, doi: 10.1080/21870764.2022.2127504.
- [31] S. Navale, M. Shahbaz, A. Mirzaei, S. S. Kim, and H. W. Kim, "Effect of ag addition on the gas-sensing properties of nanostructured resistive-based gas sensors: An overview," *Sensors*, vol. 21, no. 19, MDPI, Oct. 01, 2021, doi: 10.3390/s21196454.
- [32] M. Aleksanyan, A. Sayunts, V. Aroutiounian, G. Shahkhatuni, Z. Simonyan, and G. Shahnazaryan, "Gas Sensor Based on ZnO Nanostructured Film for the Detection of Ethanol Vapor," *Chemosensors*, vol. 10, no. 7, Jul. 2022, doi: 10.3390/chemosensors10070245.
- [33] V. S. Bhati, M. Hojamberdiev, and M. Kumar, "Enhanced sensing performance of ZnO nanostructures-based gas sensors: A review," *Energy Reports*, vol. 6, Elsevier Ltd, pp. 46–62, Feb. 01, 2020, doi: 10.1016/j.egy.2019.08.070.
- [34] S. Pati, A. Maity, P. Banerji, and S. B. Majumder, "Temperature dependent donor-acceptor transition of ZnO thin film gas sensor during butane detection," *Sens Actuators B Chem*, vol. 183, pp. 172–178, 2013, doi: 10.1016/j.snb.2013.03.120.